$L_{2,3}M_{4,5}M_{4,5}$ x-ray-excited Auger-electron spectra of In, Sn, and Sb

G. G. Kleiman, R. Landers, P. A. P. Nascente,* and S. G. C. de Castro
Departamento de Física Aplicada, Instituto de Física "Gleb Wataghin," Universidade Estadual de Campinas, Caixa Postal 6165, 13081 Campinas, São Paulo, Brazil
(Received 7 January 1992)

$L_{2,3}M_{4,5}M_{4,5}$ Auger spectra have been investigated for clean samples of In, Sn, and Sb using bremsstrahlung for excitation. The experimental spectra are in good agreement with atomic-multiplet-structure calculations in which the initial state is treated in the *jj* and the final state in the intermediate-coupling scheme.

I. INTRODUCTION

Much of the interest in x-ray-excited Auger-electron spectroscopy (XAES) of noble and transition metals and their alloys have revolved around the transitions involving final-state *d*-band holes (i.e., *iVV* transitions). The reason for a great deal of this interest is that these spectra yield information about the two-hole density of states, which clarifies hole-hole Coulomb interaction and correlation effects, for example.

Transitions involving only core levels (i.e., *ijk* transitions) have received much less attention. One reason is that they do not yield a wealth of valence-band information such as that afforded by the *iVV* spectra. Nevertheless, their study is interesting for a number of reasons, such as the following. (1) Theories of Auger energies assume self-consistent screening of core holes[1,2] so that their predictions should be compared to the results of measurements of *ijk* spectra. (2) Shifts of Auger energies, which offer information complementary to that of binding-energy shifts of x-ray photoelectron spectra, should be measured from *ijk* spectra, since corresponding shifts of *iVV* spectra may be affected by the density of states, even when the *iVV* spectra are of quasiatomic origin.[3] (3) Comparison with spectra calculated from atomic theories indicate the validity of these theories and permit comparison of the theoretical parameters so determined with those of the corresponding atoms, elucidating, in this way, solid-state effects.

Reports of such high-resolution spectra in the literature are few, however. Usually, such spectra are either broad, partially as a result of the superposition of contributions from various terms, as in the case of the $L_{2,3}M_{2,3}M_{2,3}$ spectra of the $3d$ series[4] and the $N_{6,7}O_{4,5}O_{4,5}$ spectra of Tl, Pb, and Bi,[5] or they are weak in intensity and of very high kinetic energies, as in the case of the $L_{2,3}M_{4,5}M_{4,5}$ spectra of the $4d$ series.[6–9] For these reasons, it is not common to experimentally study Auger transitions involving only core levels.

Comparisons of the results of atomic calculations and high-resolution *LMM* Auger measurements for the $3d^4$ and $5d^5$ metals have been discussed in detail in the literature. Such spectra for the $4d$ metals have recently been reported.[8,9] These are sufficiently narrow and simple in form, even though weak, to permit an unambiguous evaluation of the theoretical agreement.

In this paper, we report the experimental $L_2M_{4,5}M_{4,5}$ and $L_3M_{4,5}M_{4,5}$ Auger spectra of In, Sn, and Sb. We also present the transition probabilities for all the final-state terms in these Auger processes in both the *jj-LS* and *jj*-intermediate coupling schemes[5] for the initial and final states. We also determine the term splittings in these materials. As in the case of the $3d$ $L_{2,3}M_{4,5}M_{4,5}$ spectra,[4] a satisfactory agreement between theory and experiment is reached when the problem is considered as atomic in nature. But the *L-S* coupling scheme is much less accurate for treating the $4d$ final states than for $3d$ because of the much larger spin-orbit splitting of the $4d$ levels.

This is the first report of *jj*-intermediate coupling intensities for all of these transitions[8] and of their comparison with experiment.

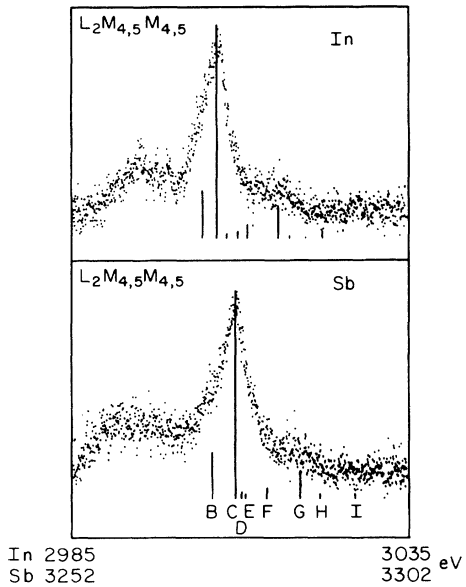

FIG. 1. $L_2M_{4,5}M_{4,5}$ Auger spectra of In and Sb with the background subtracted (Ref. 12). Our corresponding Sn spectra were too weak to be useful. The bar diagrams represent the corresponding intermediate-coupling (IC) intensities from Tables I and III. The respective experimental kinetic energies are indicated at the bottom.

II. EXPERIMENTAL PROCEDURE

Polycrystalline samples of In, Sn, and Sb were cold rolled in the form of foils. Sb was polished to a mirror finish, while the In and Sn surfaces were mechanically scraped just before mounting in a mobile carousel. The three metals were cleaned *in situ* by Ar-ion sputtering. X-ray photoelectron spectroscopy (XPS) was used to verify the cleanliness of the samples, and only amounts of oxygen so small that they were difficult to distinguish from the background were detected. The $3d$ XP spectra of all three samples were measured, and none manifested any effect of contamination.

The XAES and XPS measurements were made using an ion-pumped [base pressure of $(2-5)\times10^{-10}$ Torr] Vacuum Science Workshop (VSW) HA100 analyzer. Al $K\alpha$ ($h\nu=1486.6$ eV) and Mg $k\alpha$ ($h\nu=1253.6$ eV) were employed and the high kinetic energy (above 1500 eV) Auger spectra were excited by bremsstrahlung radiation.[10,11] Both Al and Mg anodes were operated with 15.0 mA current at 12 kV voltage. The fixed-analyzer-transmission (FAT) mode was used with a pass energy of 90.0 eV, which produces a FWHM for the Au $4f_{7/2}$ line of 1.5 eV. Details of the analyzer calibration is given elsewhere.[8,9]

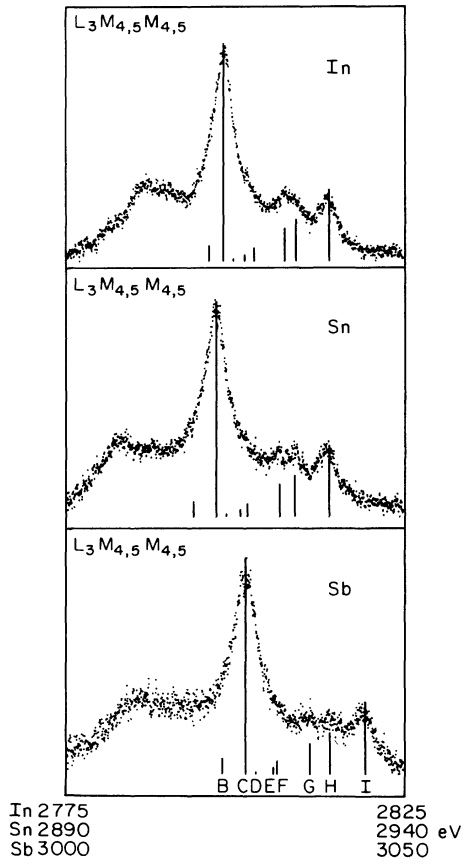

FIG. 2. $L_3M_{4,5}M_{4,5}$ Auger spectra of In, Sn, and Sb with the background subtracted (Ref. 12). The bar diagrams represent the corresponding intermediate-coupling (IC) intensities from Tables I and IV. The respective experimental kinetic energies are indicated at the bottom.

TABLE I. $L_{2,3}M_{4,5}M_{4,5}$ IC relative energies in eV. The entries in the first column correspond to the lines in Figs. 2 and 3. The indicated term is the zero spin-orbit limit of the IC state.

Term	In	Sn	Sb
A. $^1S_0$	−17.33	−18.28	−19.33
B. $^3P_2$	−2.09	−3.29	−3.40
C. $^1G_4$	0.0	0.0	0.0
D. $^3P_1$	1.48	1.49	1.49
E. $^3P_0$	3.13	3.55	4.05
F. $^1D_2$	4.50	4.57	4.62
G. $^3F_3$	9.03	9.29	9.53
H. $^3F_2$	10.72	11.57	12.52
I. $^3F_4$	15.68	16.72	17.83

III. RESULTS AND DISCUSSION

In Figs. 1 and 2, we present, respectively, the $L_2M_{4,5}M_{4,5}$ Auger spectra for In and Sb and the $L_3M_{4,5}M_{4,5}$ for In, Sn, and Sb. The spectra had the background removed by subtracting a constant fraction of the intensity integrated to higher kinetic energy than that considered.[12] The broad structures on the low-kinetic-energy sides of all the spectra in Figs. 1 and 2 appear to be in agreement with plasmon losses.[13,14]

Aside from this structure, all of the spectra exhibit several peaks whose relative energies agree with final-state term splittings. The superficial resemblance between these spectra and the corresponding ones for the $3d$ metals[4] would seem to imply that the same coupling scheme could describe them both. This is not the case, however, since the much larger $M_{4,5}$ spin-orbit separations for the elements of the $4d$ series contribute to a considerable mixing of the LS terms in the final state. Analysis of the $L_{2,3}M_{4,5}M_{4,5}$ spectra for In, Sn, and Sb requires, therefore, the use of the intermediate-coupling (IC) approximation.[15] The results of the multiplet calculations treating the final state in the IC and LS coupling schemes are presented in Tables I and II, respectively. The atomic Coulomb integrals used were those of Mann.[16] The spin-orbit parameters used in the IC calculations were 3.02, 3.36, and 3.74 eV for In, Sn, and Sb, respectively, and were derived from the experimental M_4-M_5 XPS splittings.[17]

The transition rates were also calculated in the mixed- and intermediate-coupling approximations using the radial integrals calculated by McGuire[18] for Sn, the values for In and Sb being interpolated from his tables. The results for the $L_{2,3}M_{4,5}M_{4,5}$ IC transition rates are shown in Tables III and IV, respectively, and those for the $L_{2,3}M_{4,5}M_{4,5}$ jj-LS transition rates are presented in

TABLE II. LS relative energies in eV.

Term	In	Sn	Sb
^1S	−14.77	−15.24	−15.72
^1G	0.0	0.0	0.0
^3P	2.38	2.46	2.54
^1D	3.53	3.65	3.76
^3F	9.94	10.27	10.58

TABLE III. $L_2M_{4,5}M_{4,5}$ IC relative intensities. The first column indicates the corresponding lines in Fig. 1 as well as the zero spin-orbit limit of the IC state.

Term	In	Sn	Sb
A. $^1S_0$	0.00	0.00	0.00
B. $^3P_2$	0.22	0.22	0.22
C. $^1G_4$	1.00	1.00	1.00
D. $^3P_1$	0.02	0.02	0.02
E. $^3P_0$	0.03	0.03	0.03
F. $^1D_2$	0.06	0.05	0.05
G. $^3F_3$	0.14	0.13	0.13
H. $^3F_2$	0.01	0.01	0.02
I. $^3F_4$	0.03	0.02	0.02

TABLE IV. $L_3M_{4,5}M_{4,5}$ IC relative intensities. The first column indicates the corresponding lines in Fig. 2 as well as the zero spin-orbit limit of the IC state.

A. $^1S_0$	0.00	0.00	0.00
B. $^3P_2$	0.07	0.07	0.07
C. $^1G_4$	1.00	1.00	1.00
D. $^3P_1$	0.01	0.01	0.01
E. $^3P_0$	0.03	0.03	0.03
F. $^1D_2$	0.06	0.06	0.06
G. $^3F_3$	0.15	0.15	0.14
H. $^3F_2$	0.19	0.19	0.19
I. $^3F_4$	0.33	0.34	0.33

TABLE V. $L_{2,3}M_{4,5}M_{4,5}$ *LS* relative intensities.

Term	In	Sn	Sb
^1S	0.03	0.03	0.03
^1G	1.0	1.0	1.0
^3P	0.03	0.03	0.04
^1D	0.18	0.18	0.18
^3F	0.38	0.38	0.38

TABLE VI. Eigenvectors for $4d^8$ states in intermediate coupling (J,i). The second column indicates the zero spin-orbit coupling limit of state (J,i) and the corresponding lines in Figs. 2 and 3.

$C_{Ji}(^{2S+1}L_J)$	Zero spin-orbit limit	In	Sn	Sb
$C_{01}(^1S_0)$	$^3P_0$ (*E*)	−0.92	−0.91	−0.90
$C_{01}(^3P_0)$		0.39	0.41	0.44
$C_{02}(^1S_0)$	$^1S_0$ (*A*)	0.39	0.41	0.44
$C_{02}(^3P_0)$		0.92	0.91	0.90
$C_{11}(^3P_1)$	$^3P_1$ (*D*)	1.00	1.00	1.00
$C_{21}(^3F_2)$		−0.52	−0.50	−0.48
$C_{21}(^1D_2)$	$^3F_2$ (*H*)	0.70	0.70	0.71
$C_{21}(^3P_2)$		0.49	0.51	0.53
$C_{22}(^3F_2)$		0.68	0.68	0.68
$C_{22}(^1D_2)$	$^1D_2$ (*F*)	0.00	−0.04	−0.08
$C_{22}(^3P_2)$		0.74	0.73	0.73
$C_{23}(^3F_2)$		0.51	0.53	0.56
$C_{23}(^1D_2)$	$^3P_2$ (*B*)	0.72	0.71	0.70
$C_{23}(^3P_2)$		−0.48	−0.46	−0.44
$C_{31}(^3F_3)$	$^3F_3$ (*G*)	1.00	1.00	1.00
$C_{41}(^1G_4)$	$^3F_4$ (*I*)	0.20	0.21	0.21
$C_{41}(^3F_4)$		0.98	0.98	0.98
$C_{42}(^1G_4)$	$^1G_4$ (*C*)	0.98	0.98	0.98
$C_{42}(^3F_4)$		−0.20	−0.21	−0.21

Table V. For the *jj-LS* case, the expressions used were those of Ref. 1. For the *jj*-IC calculations, the eigenvector mixing coefficients[15] corresponding to the energies in Table I are those in Table VI, and the equations used[5] are given in the Appendix.

In Figs. 1 and 2, the separations of the lines correspond to the calculated multiplet splittings, and the heights reflect the calculated relative intensities in the *jj*-IC approximation. A simple comparison of the experimental peak positions with the multiplet energies in Tables I and II indicates that the peak labeled *I* is certainly not accounted for in the *jj-LS* scheme.

In order to better demonstrate the agreement between the experimental and theoretical spectra than by the bar diagrams, in Fig. 3 we present the fittings of the data (dots) to an envelope function generated from the multiplet structure calculation (the experimental energy ranges were chosen to exclude the plasmon-loss structure in Fig. 2). To form this envelope, all the components were represented by Gaussians whose widths were constrained to be equal. The relative heights and positions were fixed

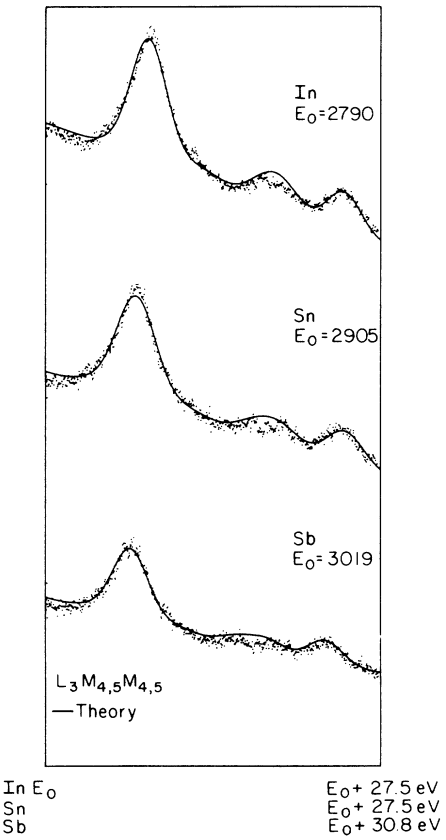

FIG. 3. $L_3M_{4,5}M_{4,5}$ Auger spectra of In, Sn, and Sb without background subtraction. The origin of each energy range is denoted by E_0; the different energy ranges are noted at the foot of the figure. Theoretical spectra corresponding to Fig. 2 are indicated by the solid curves. The background was represented by a second-order polynomial, and each component in Fig. 2 was represented by a Guassian of constant width. The widths for In, Sn, and Sb were, respectively, 3.5, 4.0, and 4.0 eV.

by the values shown in Tables IV and I. The background was supposed to be of the form of a second-order polynomial. This form approximately describes plasmon loss and other contributions to the background; the plasmon contributions were not treated explicitly because of the degree of experimental noise. The only adjustable parameters were the width and the three polynomial coefficients of the background. The widths thus obtained were 3.5, 4.0, and 4.0 eV for In, Sn, and Sb, respectively. The agreement between theory and experiment is quite good taking into account the fact that no attempt was made to optimize the Coulomb atomic integrals.

For each of the three metals, the greatest discrepancy is in the middle energy region. Whereas the theoretical curves present single broad peaks, the data appear to manifest structures with double peaks. Such a discrepancy could be eliminated by optimizing the Coulomb integrals. Because of the experimental noise and the absence of such double-peak structure in more intense spectra of $4d$ metals of lower atomic number,[20] such optimization is not necessarily meaningful.

IV. CONCLUSIONS

We report jj-LS and jj-IC multiplet structure calculations for $L_{2,3}M_{4,5}M_{4,5}$ transitions, the corresponding observed spectra for In, Sn, and Sb, as well as the comparison between theory and experiment. The agreement is generally good for the IC case and poor for LS.

The widths of the final-state components are 3.5, 4.0, and 4.0 eV for In, Sn, and Sb, respectively. These values seem to be much greater than typical atomic widths,[5] in agreement with expectations regarding lifetime reductions in the metal compared to the atom.[5]

TABLE VII. L_2-$M_{45}M_{45}$ transitions rates in jj-IC.

$J=0$	$75\lvert -C_i(^1S_0)A(0,1)+\sqrt{2}C_i(^3P_0)A(1,1)\rvert^2$
$J=1$	$\frac{675}{2}\lvert A(1,1)\rvert^2$
$J=2$	$\frac{375}{2}\lvert C_i(^3P_2)A(1,1)+\sqrt{2}C_i(^1D_2)A(2,1)\rvert^2$ $+875\left\lvert -C_i(^1D_2)A(2,3)+\frac{2}{\sqrt{3}}C_i(^3F_2)A(3,3)\right\rvert^2$
$J=3$	$\frac{15925}{12}\lvert A(3,3)\rvert^2$
$J=4$	$1575\left\lvert C_i(^1G_4)A(4,3)+\frac{\sqrt{3}}{2}C_i(^3F_4)A(3,3)\right\rvert^2$ $+2475\lvert C_i(^1G_4)A(4,5)\rvert^2$

ACKNOWLEDGMENTS

We would like to thank R. C. G. Vinhas and R. F. Suarez for technical assistance. This work was supported by CNPq, FAPESP, and FINEP of Brazil. P. A. P. Nascente thanks CNPq for financial support.

APPENDIX

The starting point of the rate calculations is the same expression given in Ref. 5 for the $n_1l_1\rightarrow(nl_3)^2$ transition rates in jj-IC coupling for an atom with closed shells prior to production of the inner shell holes,

$$\frac{w_{\rm if}}{2\pi}=2(2l_1+1)(2l_3+1)^2(2l_2+1)(2J+1)\times\sum_x(2x+1)\left|\sum_{L,S}C_i(LSJ)(-1)^L[(2L+1)(2S+1)]^{1/2}\begin{Bmatrix} l_2 & L & l_1\\ \frac{1}{2} & j_1 & x\end{Bmatrix}\begin{Bmatrix}\frac{1}{2} & S & \frac{1}{2}\\ L & x & J\end{Bmatrix}A(L,l_2)\right|^2, \tag{A1}$$

TABLE VIII. L_3-$M_{45}M_{45}$ transition rates in jj-IC.

$J=0$	$75\lvert C_i(^1S_0)A(0,1)+\frac{1}{\sqrt{2}}C_i(^3P_0)A(1,1)\rvert^2$
$J=1$	$\frac{675}{4}\lvert A(1,1)\rvert^2$
$J=2$	$5625\left[\frac{1}{6}\left\lvert -C_i(^3P_2)\frac{A(1,1)}{\sqrt{2}}+C_i(^1D_2)\frac{A(2,1)}{5}\right\rvert^2 +\frac{6}{100}\lvert C_i(^1D_2)A(2,1)\rvert^2\right]$ $+5250\left[\frac{1}{10}\lvert C_i(^1D_2)A(2,3)\rvert^2 +\frac{1}{3}\lvert C_i(^1D_2)\frac{A(2,3)}{\sqrt{5}}+C_i(^3F_2)\sqrt{5/12}A(3,3)\rvert^2\right]$.
$J=3$	$\frac{28175}{24}\lvert A(3,3)\rvert^2$
$J=4$	$\frac{525}{2}[\lvert -C_i(^3F_4)\sqrt{27/2}A(3,3)+C_i(^1G_4)A(4,3)\rvert^2$ $+5\lvert C_i(^1G_4)A(4,3)\rvert^2]$ $+2475\lvert C_i(^1G_4)A(4,5)\rvert^2$

$$A(L,l_2)=\sum_k \begin{bmatrix} l_1 & l_3 & k \\ l_3 & l_2 & L \end{bmatrix} \begin{bmatrix} l_1 & k & l_3 \\ 0 & 0 & 0 \end{bmatrix} \begin{bmatrix} l_2 & k & l_3 \\ 0 & 0 & 0 \end{bmatrix} (2k+1)D(k,l_2) , \tag{A2}$$

where $A(L,l_2)\neq 0$ only when $S+L$ is even and the brackets denote the $6j$ and $3j$ symbols.[19] $C_i(LSJ)$ is an intermediate-coupling mixing coefficient. The C's for the $L_{2,3}M_{4,5}M_{4,5}$ transition are presented in Table VI.

The radial matrix element is taken to be

$$D(k,l_2)=\frac{1}{2k+1}\int dr_1 \int dr_2 \phi_{2p}(r_1)\phi_{l_2}(r_2) \left[\frac{(r_<)^k}{(r_>)^{k+1}} \right] \phi_{4d}(r_1)\phi_{4d}(r_2) . \tag{A3}$$

The evaluation of the transition rates for the $L_{2,3}M_{4,5}M_{4,5}$ produces the expressions listed in Tables VII and VIII. The specific expressions for the $A(L,l_2)$ are given in Eqs. (A4)–(A10),

$$A(0,1)=\tfrac{1}{5}\sqrt{1/15}[2D(1,1)+3D(3,1)] , \tag{A4}$$

$$A(1,1)=\tfrac{1}{5}\sqrt{1/5}[D(3,1)-D(1,1)] , \tag{A5}$$

$$A(2,1)=\tfrac{1}{25}[\sqrt{7/3}D(1,1)+\sqrt{3/7}D(3,1)] , \tag{A6}$$

$$A(2,3)=-\tfrac{1}{175}\sqrt{6}[D(1,3)+4D(3,3)] , \tag{A7}$$

$$A(3,3)=\tfrac{1}{35}\sqrt{6/5}[D(1,3)-D(3,3)] , \tag{A8}$$

$$A(4,3)=-\tfrac{3}{35}\sqrt{2/5}[D(1,3)+\tfrac{1}{9}D(3,3)] , \tag{A9}$$

$$A(4,5)=\tfrac{1}{3}\sqrt{2/77}D(3,5) . \tag{A10}$$

*Also at the Laboratório Nacional de Luz Sincrotron, Rua Lauro Vanucci 1020, 13085 Campinas, São Paulo, Brazil.

[1]B. Johansson and N. Mårtensson, Phys. Rev. B **21**, 4427 (1980).
[2]N. D. Lang and A. R. Williams, Phys. Rev. B **16**, 2408 (1977).
[3]G. G. Kleiman, R. Landers, S. G. C. de Castro, and P. A. P. Nascente, Phys. Rev. B **45**, 13 899 (1992).
[4]E. Antonides, E. C. Janses, and G. A. Sawatzky, Phys. Rev. B **15**, 1669 (1977).
[5]J. F. McGilp, P. Weightman, and E. J. McGuirre, J. Phys. C **10**, 3445 (1977).
[6]G. G. Kleiman, R. Landers, S. G. C. de Castro, and P. A. P. Nascente, Phys. Rev. B **44**, 3383 (1991).
[7]G. G. Kleiman, R. Landers, S. G. C. de Castro, and P. A. P. Nascente, J. Vac. Sci. Technol. A (to be published).
[8]G. G. Kleiman, R. Landers, P. A. P. Nascente, and S. G. C. de Castro, Phys. Rev. B (to be published).
[9]R. Landers, P. A. P. Nascente, S. G. C. de Castro, and G. G. Kleiman, J. Phys. Condens. Matter (to be published).
[10]C. D. Wagner and J. A. Taylor, J. Electron Spectrosc. Relat. Phenom. **20**, 83 (1980).
[11]V. S. Sundaram, J. D. Rogers, and R. Landers, J. Vac. Sci. Technol. **A19**, 117 (1981).
[12]D. A. Shirley, Phys. Rev. B **5**, 4709 (1972).
[13]A. C. Parry-Jones, P. Weightman, and P. T. Andrews, J. Phys. C **12**, 1587 (1979).
[14]R. A. Pollak, L. Ley, F. R. McFeely, S. P. Kowalczk, and D. A. Shirley, J. Electron Spectrosc. Relat. Phenom. **3**, 381 (1974).
[15]E. U. Condon and G. H. Shortley, *The Theory of Atomic Spectra* (Cambridge University, London, 1963).
[16]J. B. Mann, Los Alamos Scientific Laboratory Report No. LASL-3690, 1967 (unpublished).
[17]R. Nyholm and N. Mårtensson, J. Phys. C **13**, L279 (1980).
[18]E. J. McGuirre, Sandia Laboratory Report No. SC-RR-710075, 1971 (unpublished).
[19]M. Rotemberg, *The* $3-j$ *and* $6-j$ *Symbols* (Lockwood, London, 1959).
[20]S. G. C. de Castro, G. G. Kleiman, R. Landers, and P. A. P. Nascente (unpublished).